Acta Cryst E CRYSTALLOGRAPHIC COMMUNICATIONS

ISSN 2056-9890

Synthesis and crystal structure of 1,1′-bis{[4-(pyridin-2-yl)-1,2,3-triazol-1-yl]methyl}ferrocene, and its complexation with Cu^{I}

Uttam R. Pokharel,[a]* Aaron P. Naquin,[a] Connor P. Brochon[a] and Frank R. Fronczek[b]

[a]Department of Chemistry & Physical Sciences, Nicholls State University, Thibodaux, Louisiana 70301, USA, and [b]Department of Chemistry, Louisiana State University, Baton Rouge, Louisiana, 70803, USA. *Correspondence e-mail: uttam.pokharel@nicholls.edu

Received 5 August 2020
Accepted 28 August 2020

Edited by S. Parkin, University of Kentucky, USA

Keywords: 1,1′-bis(pyridyltriazoylmethyl)ferrocene; crystal structure; click reaction; tetradentate ligand; disubstituted ferrocene; copper(I) complex.

CCDC reference: 2026000

Supporting information: this article has supporting information at journals.iucr.org/e

The title compound, $[Fe(C_{13}H_{11}N_4)_2]$, was synthesized starting from 1,1′-ferrocenedicarboxylic acid in a three-step reaction sequence. The dicarboxylic acid was reduced to 1,1′-ferrocenedimethanol using $LiAlH_4$ and subsequently converted to 1,1′-bis(azidomethyl)ferrocene in the presence of NaN_3. The diazide was treated with 2-ethynylpyridine under 'click' conditions to give the title compound in 75% yield. The Fe^{II} center lies on an inversion center in the crystal. The two pyridyltriazole wings are oriented in an *anti* conformation and positioned *exo* from the Fe^{II} center. In the solid state, the molecules interact by C—H···N, C—H···π, and π–π interactions. The complexation of the ligand with $[Cu(CH_3CN)_4](PF_6)$ gives a tetranuclear dimeric complex.

1. Chemical context

Metal–organic supramolecular chemistry is an emerging area in inorganic chemistry: the structurally challenging functional supramolecules can be constructed from the self-assembly of multidentate organic ligands and transition-metal ions in relatively few synthetic steps (Cook & Stang, 2015). Such supramolecules are designed by careful selection of the conformational flexibility of the linker groups in multidentate ligands, and the coordination preference of transition-metal ions. We have recently studied the self-assemblies of *m*-xylylene- or 2,7-naphthalenebis(methylene)-bridged tetradentate bis(pyridyltriazole) ligands with Cu^{II} ions to give discrete [2 + 2] metallocycles (Pokharel *et al.*, 2013, 2014). In a continuation of our work, we became interested in the design of metalloligands, *i.e.*, metal-containing organic linkers, to produce mixed-metal complexes with different topologies.

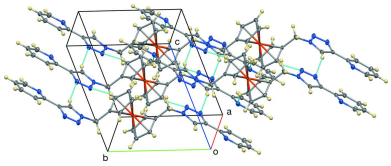

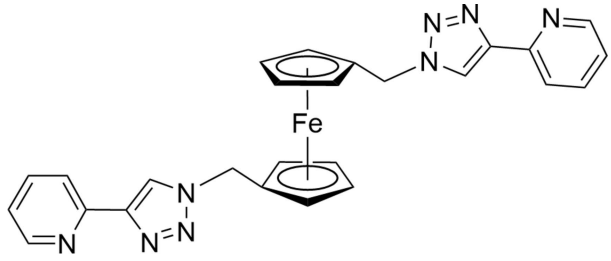

Ferrocene, a well-known metallocene, exhibits high thermal stability, reversible electrochemistry, and conformational flexibility, making it an ideal precursor for the development of polymetallic metallosupramolecular complexes (Astruc, 2017). Introduction of the iron(II) center as the structural

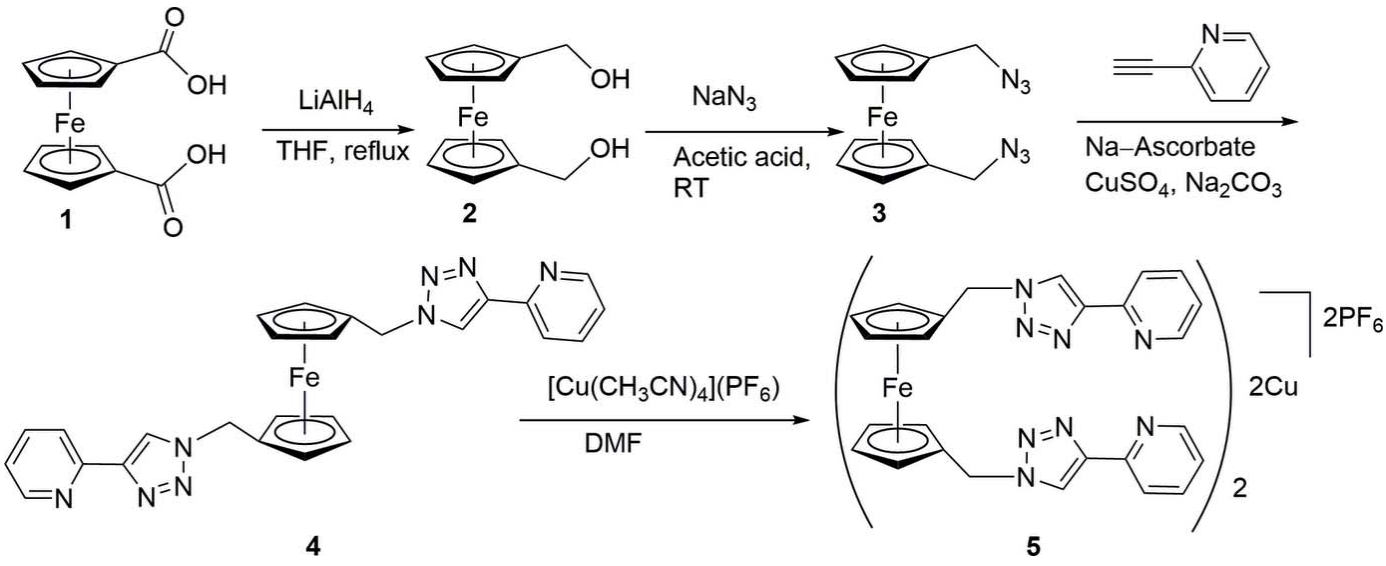

Figure 1
The synthetic scheme showing the formation of the title compound and its complexation with Cu^{I}.

component of the ligand allows the study of electronic coupling between metal centers in heterometallic metallosupramolecular assemblies. Although 1,1′-disubstituted ferrocenes featuring the pyridyl moiety as a donor group have been exploited in metallosupramolecular assemblies (Quinodoz *et al.*, 2004; Buda *et al.*, 1998; Ion *et al.*, 2002; Lindner *et al.*, 2003; Sachsinger & Hall, 1997), the ferrocene-bridged bis(pyridyltriazole)-based tetradentate ligands are relatively new in coordination chemistry (Findlay *et al.*, 2018; Manck *et al.*, 2017; Romero *et al.*, 2011). Herein, we report the synthesis of the 1,1′-bis(methylenepyridyltriazole) ferrocene ligand starting from 1,1′-ferrocenedicarboxylic acid in a three-step sequence and its complexation with Cu^{I} ions (Fig. 1).

1,1′-Ferrocenedimethanol, **2**, was synthesized by reduction of 1,1′-ferrocenedicarboxylic acid, **1**, in the presence of $LiAlH_4$. The diol was treated with sodium azide in acetic acid following published procedures (Casas-Solvas *et al.*, 2009) to give 1,1′-bis(azidomethyl)ferrocene, **3** as a viscous liquid. The compound showed a strong IR absorption at 2093 cm^{-1}, indicating the formation of the desired diazide (Casas-Solvas *et al.*, 2009). The diazide was treated with 2-ethynylpyridine under 'click' conditions (Pokharel *et al.*, 2013) to give the title compound in 75% yield. This new tetradentate ligand based on ferrocene is obtained as an air-stable light-brown crystalline powder.

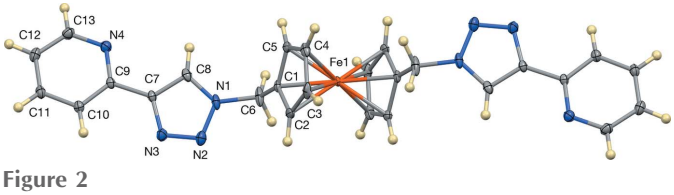

Figure 2
Molecular structure of the title compound showing the atom-numbering scheme. Displacement ellipsoids are drawn at the 50% probability level. Unlabeled atoms are generated by the symmetry operation $1 - x, 1 - y, 1 - z$.

2. Structural commentary

The asymmetric unit of the title compound contains one half of the molecule since the Fe^{II} center is on an inversion center, as shown in Fig. 2. The symmetry in the molecule was also apparent in the NMR data where only one set of signals was found for the protons and carbons of the cyclopentadienyl (Cp) rings, methylene groups, and the pyridyltriazole units. The Fe—C(Cp) bond lengths are in the range 2.0349 (12)–2.0471 (13) Å [average 2.0498 (13) Å] with the Fe···Cp-centroid distance being 1.6550 (6) Å. The Fe—C bond to the substituted carbon [Fe—C1 2.0349 (12)] is shorter than the remaining Fe—C bond lengths, as is seen in similar 1,1′-disubstituted ferrocene derivatives (Glidewell *et al.*, 1994). The conformation of the ferrocenyl unit is exactly staggered by inversion symmetry, and the centrosymmetry also makes the Cp—Fe—Cp linkage linear and the Cp rings parallel. The Csp^3 atom, C6, is displaced towards the Fe^{II} center by 0.044 (3) Å from the least-squares plane of the Cp ring. The C_{Cp}—Csp^3 and C_{Cp}—N bond lengths involving C6 are 1.4910 (19) and 1.4700 (18) Å, respectively. The pyridyltriazole moiety is oriented *exo* from the Fe^{II} center, with the least-squares planes of the Cp and triazole rings forming a dihedral angle of 65.68 (5)°. The nitrogen donor atoms of the pyridyltriazole units adopt an *anti* conformation, as is often observed in this type of chelating ligand (Crowley & Bandeen, 2010). The pyridyl and triazole units deviate slightly from coplanarity, with the N3—C7—C9—N4 torsion angle being 167.64 (13)°.

3. Supramolecular features

The crystal structure of the title compound is consolidated by intermolecular C—H···N (Table 1), C—H···π, and π–π interactions (Figs. 3 and 4). The triazole carbon C8 forms a C—H···N interaction, with a C···N distance of 3.601 (2) Å to

Table 1
Hydrogen-bond geometry (Å, °).

D—H···A	D—H	H···A	D···A	D—H···A
C8—H8···N3^{i}	0.95	2.68	3.601 (2)	163
C5—H5···N2^{i}	0.95	2.51	3.4240 (19)	160
C3—H3···N4^{ii}	0.95	2.73	3.4625 (19)	135
C12—H12···Cp$_{centroid}$^{iii}	0.95	2.69	3.4861 (15)	142

Symmetry codes: (i) $x-1, y, z$; (ii) $x, y+1, z$; (iii) $-x+2, -y, -z$.

triazole N3 (at $x-1, y, z$) and the Cp carbon atom C5 forms a C—H···N interaction with a C···N distance of 3.4240 (19) Å to triazole N2 (at $x-1, y, z$). These two contacts form a ring with graph-set motif $R_2^2(9)$ (Etter *et al.*, 1990). In addition, the triazole carbon C3 forms a C—H···N interaction with a C···N distance of 3.4625 (19) Å to pyridyl nitrogen N4 (at $x, y+1, z$). Thus, the C—H···N contacts form a two-dimensional network normal to [001]. The pyridyltriazole moieties stack in an *anti*-parallel fashion about inversion centers. The pyridyl moiety of one molecule has a π–π interaction with the triazole moiety of another molecule with a dihedral angle of 11.27 (10)° and centroid–centroid distance of 3.790 Å (symmetry operation $2-x, -y, -z$). In addition, there are also C—H···π interactions between the hydrogen atom of the pyridyl moiety with the cyclopentadienyl ring [H12···Cp(centroid) = 2.692 Å; symmetry operation $2-x, -y, -z$;]. These two interactions thus form centrosymmetric dimers, illustrated in Fig. 4.

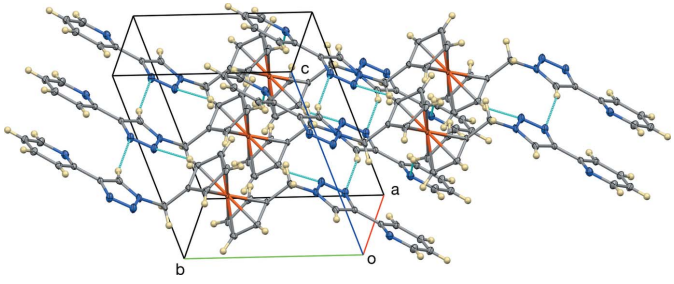

Figure 3
The C—H···N network, with displacement ellipsoids at the 50% probability level.

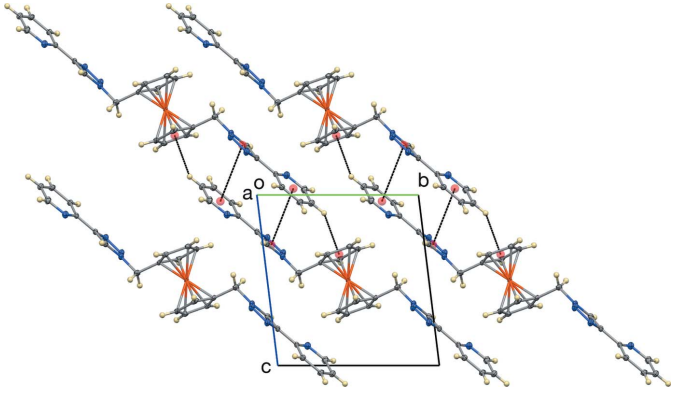

Figure 4
The C—H···π and π–π interactions, viewed along the *a* axis. Displacement ellipsoids are shown at the 50% probability level.

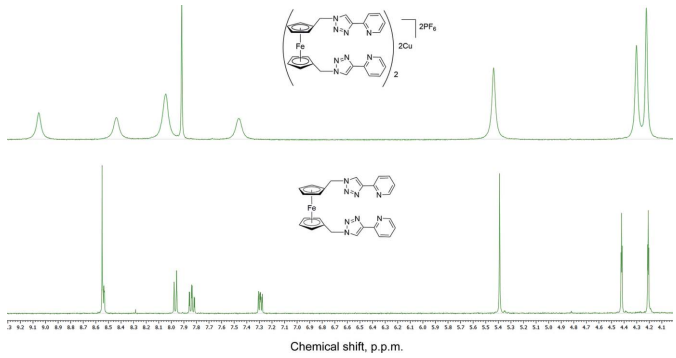

Figure 5
^{1}H NMR spectra of ligand **4** (bottom) and its Cu^{I} complex, **5** (top). Both spectra are clipped on the same chemical shift ranges.

4. Database survey

A search of the Cambridge Structural Database (Version 5.41, update of March 2020; Groom *et al.*, 2016) for bis(pyridyltriazole) with a ferrocene linker gave no results. However, the structure of ferrocene attached to one methylenepyridyltriazole, BULQIJ (Crowley *et al.*, 2010) has been reported. The two pyridyltriazole units connected with organic linkers, namely *m*-xylylene, VAJVIN (Najar *et al.*, 2010), and *p*-xylylene as chloroform solvate, FUJJOK (Crowley & Bandeen, 2010) have also been reported.

5. Complexation with Cu^{I}

Complexation of the ligand **4** with Cu^{I} was performed under a nitrogen atmosphere. When $[Cu(CH_3CN)_4]PF_6$ was added to a suspension of the ligand in DMF in a 1:1 ratio, the mixture was completely soluble, indicating the formation of a complex. To avoid oxidation of the complex, the resultant solution was diffused with diethyl ether vapor under nitrogen for 3 d. Under these conditions, a bright-yellow microcrystalline solid was formed. At room temperature, the ^{1}H NMR spectrum of the complex showed a simple pattern containing the same set of signals for the ligand, indicative of the presence of one single species in solution. Compared to the spectrum of the free ligand, the proton signals of the complex, especially for

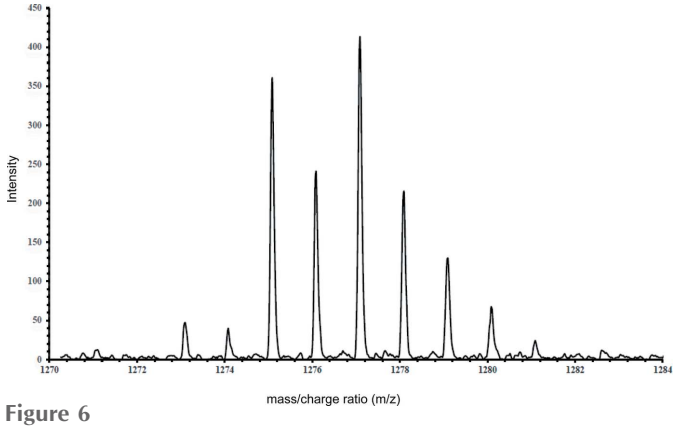

Figure 6
A portion of the high-resolution ESI–MS spectrum of complex **5**

the pyridyltriazole coordination pocket, are shifted downfield (Fig. 5). Similar retaining of the number of signals and the coupling patterns in the ^{1}H NMR spectrum was observed in xylylene-linked bis(pyridyltriazole) ligands and their Ag^I complexes (Crowley & Bandeen, 2010). To further explore the nature of the complex in solution, we examined a MeOH/DMSO solution of the complex by positive-ion electrospray mass spectrometry (ESMS). The ESMS spectrum of the complex contains a peak at 1273.0915 corresponding to $[Cu_2L_2](PF_6)^+$ with a similar isotopic pattern as the theoretical simulation (Fig. 6), indicating the formation of the [2 + 2] complex. Disappointingly, despite obtaining crystalline material, our attempts to obtain crystals suitable for single-crystal X-ray analysis failed.

6. Synthesis and crystallization

Synthesis of 1,1′-bis(hydroxymethyl)ferrocene, 2. To a stirred solution of 1,1′-ferrocenedicarboxylic acid (4.00 g, 14.59 mmol) in dry THF (400.0 mL), 1.0 *M* $LiAlH_4$ (58.38 mL, 58.38 mmol) was added dropwise at room temperature under N_2. The reaction vigorously produced hydrogen gas. The reaction mixture was refluxed for 2 h, by which time the starting compound was consumed, as evidenced by TLC. The reaction was again cooled to room temperature, and ethyl acetate (5 mL) and water (10 mL) were added in sequence with constant stirring. The product was extracted with ethyl acetate (4 × 150 mL). The combined organic layer was dried with anhydrous $MgSO_4$ and volatiles removed *in vacuo* to give **2** (3.46 g, 96%) as a brown solid. The analytically pure product was obtained by recrystallization from toluene upon cooling. ^{1}H NMR (acetone-d_6, 400 MHz, ppm): δ 4.07 (*t*, 4H, ^3J = 1.6 Hz, Cp), 4.13 (*t*, 4H, ^3J = 1.6 Hz, Cp), 4.19 (*t*, 2H, ^3J = 6.0 Hz, OH), 4.30 (*d*, 4H, ^3J = 6.0 Hz, CH_2). ^{13}C NMR (acetone-d_6, 100 MHz, ppm): δ 67.4, 67.7, 69.6, 89.7.

Synthesis of 1,1′-bis(azidomethyl)ferrocene, 3. Caution! Organic azides with low C/N ratio are potentially dangerous. However, we did not encounter any problem during the synthesis of diazide and its subsequent derivatization. To a stirred solution of 1,1′-hydroxymethylferrocene (1.50 g, 6.09 mmol) in glacial acetic acid (7.5 mL), sodium azide (2.23 g, 36.5 mmol) was added. The reaction was stirred for 3 h at 323 K under nitrogen. The reaction mixture was neutralized with a saturated solution of sodium bicarbonate. The product was extracted with chloroform (2 × 50 mL). The organic phase was dried with anhydrous $MgSO_4$ and the volatiles removed *in vacuo* to give **3** (1.50 g, 83%) as a viscous liquid. IR (ATR, cm^{-1}): 2092 (*s*), 1733 (*w*), 1240 (*m*). ^{1}H NMR ($CDCl_3$, 400 MHz, ppm): δ 4.10 (*s*, 4H, CH_2), 4.19 (*t*, ^3J = 2.0 Hz, Cp), 4.22 (*t*, ^3J = 2.0 Hz, Cp).

Synthesis of 1,1′-bis(pyridyltriazolylmethyl)ferrocene, 4. To a stirred solution of 1,1′-bis(azidomethyl)ferrocene (1.00 g, 3.34 mmol) in a mixture of DMF and water (4:1) (20 mL), Na_2CO_3 (354 mg, 3.34 mmol), $CuSO_4{\cdot}5H_2O$ (333 mg, 1.33 mmol), ascorbic acid (468 mg, 2.66 mmol), and 2-ethynylpyridine (862 mg, 8.36 mmol) were added in sequence. The reaction mixture was stirred for 20 h at room temperature, and then poured into an NH_3/EDTA solution (2.00 g of $Na_2H_2EDTA{\cdot}2H_2O$ in 5 mL of 28% aqueous NH_3, diluted to 100 mL with H_2O) and the mixture extracted with chloroform (3 x 100 mL). The organic layer was collected, dried over $MgSO_4$, and evaporated to dryness. The crude product was purified by trituration with cold diethyl ether to give **4** (1.26 g, 75%) as a light-brown solid. X-ray quality crystals of the compound were obtained by vapor diffusion of diethyl ether into its solution in chloroform, m.p.: decomposes above 463 K. ^{1}H NMR ($CDCl_3$, 400 MHz, ppm): δ 4.24 (*t*, 4H, ^3J = 2.0 Hz, Cp), 4.32 (*t*, 4H, ^3J = 2.0 Hz, Cp), 5.33 (*s*, 4H, CH_2),7.21(*td*, 2H, ^3J = 5.2 Hz, ^4J = 2.0 Hz, Ar), 7.75 (*td*, 2H, ^3J = 8.0 Hz, ^4J = 2.0 Hz, Ar), 8.05 (*s*, 2H, triazole-H), 8.15 (*d*, 2H, ^3J = 7.6 Hz, Ar), 8.53 (*d*, 2H, ^3J = 4.0 Hz, Ar) ^{13}C NMR ($CDCl_3$, 100 MHz, ppm): δ 49.8, 69.8, 70.2, 81.9, 120.3, 121.5, 122.9, 137.0, 148.4, 149.4, 150.2. HRESI–MS: *m*/*z* = 501.1416 [**4**+H]$^+$ (calculated for $C_{26}H_{23}FeN_8$ 501.1442), 523.1238 [**4**+Na]$^+$ (calculated for $C_{26}H_{23}FeN_8$ 523.1261).

Synthesis of Cu^I complex of 1,1′-bis(pyridyltriazolylmethyl)ferrocene, 5. To a nitrogen-purged stirred suspension of **4** (100 mg, 0.20 mmol) in DMF (10 mL), $[Cu(CH_3CN)_4](PF_6)$ (77 mg, 0.20 mmol) was added. The reaction produced a clear yellow solution, which was stirred for 2 h at room temperature. The reaction mixture was diffused with nitrogen-purged diethyl ether using a cannula for 3 d. The solution was decanted and the product was washed with diethyl ether and dried under a slow stream of nitrogen to give **5** (142 mg, 100%) as a yellow microcrystalline solid. A ^{1}H NMR sample was prepared by dissolving the compound in DMSO-d_6 and transferring the solution into an NMR tube under nitrogen. ^{1}H NMR (DMSO-d_6, 400 MHz, ppm): δ 4.21 (*br*, 8H, Cp), 4.29 (*br*, 8H, Cp), 5.43 (*s*, 5.42, 8H, CH_2, 7.45 (*br*, 4H, Ar), 7.90 (*s*, 4H, triazole-H), 8.04 (*br*, 4H, Ar), 8.43 (*br*, 4H, Ar), 9.05 (*br*, 4H, Ar). HRESI–MS: *m*/*z* = 1273.0915 $(Cu_2\mathbf{4}_2](PF_6)^+$ (calculated for $C_{52}H_{44}Cu_2F_6Fe_2N_{16}P$ 1273.0914), 563.0650 [Cu**4**](PF$_6$)$^+$ (calculated for $C_{26}H_{22}CuFeN_8$ 563.0660).

7. Refinement

Crystal data, data collection and structure refinement details are summarized in Table 2. All H atoms were located in difference maps and then treated as riding in geometrically idealized positions with C—H distances of 0.95 Å (0.99 Å for CH_2) and with U_{iso}(H) =1.2U_{eq} for the attached C atom.

Acknowledgements

The authors are grateful to the Department of Chemistry, Louisiana State University for providing access to single-crystal X-ray analysis of the reported compound without any cost.

Funding information

Funding for this research was provided by: Nicholls Research Council, Nicholls State University (USA) (grant to Uttam Pokharel).

Table 2
Experimental details.

Crystal data	
Chemical formula	$[Fe(C_{13}H_{11}N_4)_2]$
M_r	502.36
Crystal system, space group	Triclinic, $P\overline{1}$
Temperature (K)	90
a, b, c (Å)	5.7905 (3), 9.7461 (5), 10.1720 (4)
α, β, γ (°)	82.064 (3), 84.754 (4), 77.739 (4)
V (Å^3)	554.44 (5)
Z	1
Radiation type	Mo $K\alpha$
μ (mm^{-1})	0.71
Crystal size (mm)	0.12 × 0.09 × 0.08
Data collection	
Diffractometer	Bruker Kappa APEXII DUO CCD
Absorption correction	Multi-scan (*SADABS*; Krause *et al.*, 2015)
T_{min}, T_{max}	0.857, 0.945
No. of measured, independent and observed [$I > 2\sigma(I)$] reflections	7058, 4199, 3569
R_{int}	0.020
(sin $\theta/\lambda)_{max}$ (Å^{-1})	0.769
Refinement	
$R[F^2 > 2\sigma(F^2)]$, $wR(F^2)$, S	0.041, 0.099, 1.06
No. of reflections	4199
No. of parameters	160
H-atom treatment	H-atom parameters constrained
$\Delta\rho_{max}$, $\Delta\rho_{min}$ (e Å^{-3})	0.98, −0.29

Computer programs: *APEX3* and *SAINT* (Bruker, 2016), *SHELXS97* (Sheldrick, 2008), *SHELXL2014/7* (Sheldrick, 2015), *Mercury* (Macrae *et al.*, 2020) and *publCIF* (Westrip, 2010).

References

Astruc, D. (2017). *Eur. J. Inorg. Chem.* **2017**, 6–29.
Bruker (2016). *APEX2* and *SAINT*. Bruker AXS Inc., Madison, Wisconsin, USA.
Buda, M., Moutet, J.-C., Saint-Aman, E., De Cian, A., Fischer, J. & Ziessel, R. (1998). *Inorg. Chem.* **37**, 4146–4148.
Casas-Solvas, J. M., Ortiz-Salmerón, E., Giménez-Martínez, J. J., García-Fuentes, L., Capitán-Vallvey, L. F., Santoyo-González, F. & Vargas-Berenguel, A. (2009). *Chem. Eur. J.* **15**, 710–725.
Cook, T. R. & Stang, P. J. (2015). *Chem. Rev.* **115**, 7001–7045.
Crowley, J. D. & Bandeen, P. H. (2010). *Dalton Trans.* **39**, 612–623.
Crowley, J. D., Bandeen, P. H. & Hanton, L. R. (2010). *Polyhedron*, **29**, 70–83.
Etter, M. C., MacDonald, J. C. & Bernstein, J. (1990). *Acta Cryst.* B**46**, 256–262.
Findlay, J. A., McAdam, C. J., Sutton, J. J., Preston, D., Gordon, K. C. & Crowley, J. D. (2018). *Inorg. Chem.* **57**, 3602–3614.
Glidewell, C., Zakaria, C. M., Ferguson, G. & Gallagher, J. F. (1994). *Acta Cryst.* C**50**, 233–238.
Groom, C. R., Bruno, I. J., Lightfoot, M. P. & Ward, S. C. (2016). *Acta Cryst.* B**72**, 171–179.
Ion, A., Buda, M., Moutet, J.-C., Saint-Aman, E., Royal, G., Gautier-Luneau, I., Bonin, M. & Ziessel, R. (2002). *Eur. J. Inorg. Chem.* pp. 1357–1366.
Krause, L., Herbst-Irmer, R., Sheldrick, G. M. & Stalke, D. (2015). *J. Appl. Cryst.* **48**, 3–10.
Lindner, E., Zong, R., Eichele, K., Weisser, U. & Ströbele, M. (2003). *Eur. J. Inorg. Chem.* pp. 705–712.
Macrae, C. F., Sovago, I., Cottrell, S. J., Galek, P. T. A., McCabe, P., Pidcock, E., Platings, M., Shields, G. P., Stevens, J. S., Towler, M. & Wood, P. A. (2020). *J. Appl. Cryst.* **53**, 226–235.
Manck, S., Röger, M., van der Meer, M. & Sarkar, B. (2017). *Eur. J. Inorg. Chem.* pp. 477–482.
Najar, A. M., Tidmarsh, I. S. & Ward, M. D. (2010). *CrystEngComm*, **12**, 3642–3650.
Pokharel, U. R., Fronczek, F. R. & Maverick, A. W. (2013). *Dalton Trans.* **42**, 14064–14067.
Pokharel, U. R., Fronczek, F. R. & Maverick, A. W. (2014). *Nat. Commun.* **5**, 5883.
Quinodoz, B., Labat, G., Stoeckli-Evans, H. & von Zelewsky, A. (2004). *Inorg. Chem.* **43**, 7994–8004.
Romero, T., Orenes, R. A., Espinosa, A., Tárraga, A. & Molina, P. (2011). *Inorg. Chem.* **50**, 8214–8224.
Sachsinger, N. & Hall, C. D. (1997). *J. Organomet. Chem.* **531**, 61–65.
Sheldrick, G. M. (2008). *Acta Cryst.* A**64**, 112–122.
Sheldrick, G. M. (2015). *Acta Cryst.* C**71**, 3–8.
Westrip, S. P. (2010). *J. Appl. Cryst.* **43**, 920–925.

supporting information

Acta Cryst. (2020). E**76**, 1582-1586 [https://doi.org/10.1107/S2056989020011901]

Synthesis and crystal structure of 1,1′-bis{[4-(pyridin-2-yl)-1,2,3-triazol-1-yl]methyl}ferrocene, and its complexation with Cu^{I}

Uttam R. Pokharel, Aaron P. Naquin, Connor P. Brochon and Frank R. Fronczek

Computing details

Data collection: *APEX3* (Bruker, 2016); cell refinement: *SAINT* (Bruker, 2016); data reduction: *SAINT* (Bruker, 2016); program(s) used to solve structure: *SHELXS97* (Sheldrick, 2008); program(s) used to refine structure: *SHELXL2014/7* (Sheldrick, 2015); molecular graphics: *Mercury* (Macrae *et al.*, 2020); software used to prepare material for publication: *publCIF* (Westrip, 2010).

1,1′-Bis{[4-(pyridin-2-yl)-1,2,3-triazol-1-yl]methyl}ferrocene

Crystal data

$[Fe(C_{13}H_{11}N_4)_2]$
M_r = 502.36
Triclinic, $P\overline{1}$
a = 5.7905 (3) Å
b = 9.7461 (5) Å
c = 10.1720 (4) Å
α = 82.064 (3)°
β = 84.754 (4)°
γ = 77.739 (4)°
V = 554.44 (5) Å^3
Z = 1
$F(000)$ = 260
D_x = 1.505 Mg m^{-3}
Mo $K\alpha$ radiation, λ = 0.71073 Å
Cell parameters from 2644 reflections
θ = 3.1–33.1°
μ = 0.71 mm^{-1}
T = 90 K
Fragment, orange
0.12 × 0.09 × 0.08 mm

Data collection

Bruker Kappa APEXII DUO CCD diffractometer
Radiation source: fine-focus sealed tube
TRIUMPH curved graphite monochromator
φ and ω scans
Absorption correction: multi-scan (SADABS; Krause *et al.*, 2015)
T_{min} = 0.857, T_{max} = 0.945
7058 measured reflections
4199 independent reflections
3569 reflections with $I > 2\sigma(I)$
R_{int} = 0.020
θ_{max} = 33.2°, θ_{min} = 2.0°
h = −8→8
k = −14→14
l = −15→15

Refinement

Refinement on F^2
Least-squares matrix: full
$R[F^2 > 2\sigma(F^2)]$ = 0.041
$wR(F^2)$ = 0.099
S = 1.06
4199 reflections
160 parameters
0 restraints
Primary atom site location: structure-invariant direct methods
Secondary atom site location: difference Fourier map
Hydrogen site location: inferred from neighbouring sites
H-atom parameters constrained

$w = 1/[\sigma^2(F_o^2) + (0.0526P)^2 + 0.140P]$
where $P = (F_o^2 + 2F_c^2)/3$
$(\Delta/\sigma)_{max} < 0.001$

$\Delta\rho_{max} = 0.98$ e Å^{-3}
$\Delta\rho_{min} = -0.29$ e Å^{-3}

Special details

Geometry. All esds (except the esd in the dihedral angle between two l.s. planes) are estimated using the full covariance matrix. The cell esds are taken into account individually in the estimation of esds in distances, angles and torsion angles; correlations between esds in cell parameters are only used when they are defined by crystal symmetry. An approximate (isotropic) treatment of cell esds is used for estimating esds involving l.s. planes.

Fractional atomic coordinates and isotropic or equivalent isotropic displacement parameters (Å²)

	x	*y*	*z*	U_{iso}*/U_{eq}
Fe1	0.5000	0.5000	0.5000	0.00859 (7)
N1	0.9431 (2)	0.11300 (13)	0.36213 (12)	0.0173 (2)
N2	1.1757 (2)	0.11615 (13)	0.34215 (13)	0.0203 (2)
N3	1.2663 (2)	0.03069 (13)	0.25245 (13)	0.0175 (2)
N4	0.9549 (2)	−0.19933 (13)	0.11559 (13)	0.0166 (2)
C1	0.6904 (2)	0.34473 (13)	0.39618 (12)	0.0123 (2)
C2	0.7999 (2)	0.46543 (16)	0.37622 (14)	0.0162 (3)
H2	0.9556	0.4668	0.3976	0.019*
C3	0.6341 (3)	0.58282 (15)	0.31869 (14)	0.0186 (3)
H3	0.6595	0.6765	0.2952	0.022*
C4	0.4251 (3)	0.53559 (15)	0.30257 (13)	0.0169 (3)
H4	0.2856	0.5923	0.2663	0.020*
C5	0.4585 (2)	0.38965 (14)	0.34947 (13)	0.0132 (2)
H5	0.3458	0.3316	0.3498	0.016*
C6	0.7950 (3)	0.19952 (16)	0.45781 (15)	0.0242 (3)
H6A	0.8921	0.2067	0.5308	0.029*
H6B	0.6655	0.1517	0.4970	0.029*
C7	1.0906 (2)	−0.02744 (13)	0.21606 (13)	0.0125 (2)
C8	0.8819 (2)	0.02524 (15)	0.28631 (14)	0.0156 (2)
H8	0.7300	0.0043	0.2820	0.019*
C9	1.1331 (2)	−0.13233 (13)	0.12183 (13)	0.0119 (2)
C10	1.3477 (2)	−0.16117 (14)	0.04578 (13)	0.0141 (2)
H10	1.4713	−0.1132	0.0541	0.017*
C11	1.3757 (3)	−0.26115 (15)	−0.04177 (14)	0.0166 (3)
H11	1.5178	−0.2811	−0.0965	0.020*
C12	1.1936 (3)	−0.33183 (15)	−0.04847 (14)	0.0185 (3)
H12	1.2090	−0.4018	−0.1069	0.022*
C13	0.9891 (3)	−0.29783 (16)	0.03193 (15)	0.0187 (3)
H13	0.8656	−0.3472	0.0277	0.022*

Atomic displacement parameters (Å²)

	U^{11}	U^{22}	U^{33}	U^{12}	U^{13}	U^{23}
Fe1	0.00934 (12)	0.00722 (12)	0.00860 (12)	−0.00031 (8)	0.00181 (8)	−0.00256 (8)
N1	0.0209 (6)	0.0119 (5)	0.0147 (5)	0.0053 (4)	0.0018 (4)	−0.0026 (4)
N2	0.0243 (6)	0.0143 (5)	0.0223 (6)	−0.0015 (5)	0.0000 (5)	−0.0067 (4)

N3	0.0180 (6)	0.0138 (5)	0.0212 (6)	−0.0032 (4)	0.0011 (4)	−0.0060 (4)
N4	0.0155 (5)	0.0146 (5)	0.0198 (5)	−0.0033 (4)	−0.0001 (4)	−0.0029 (4)
C1	0.0141 (5)	0.0101 (5)	0.0108 (5)	0.0027 (4)	0.0007 (4)	−0.0033 (4)
C2	0.0120 (6)	0.0241 (7)	0.0148 (6)	−0.0060 (5)	0.0042 (4)	−0.0096 (5)
C3	0.0287 (7)	0.0127 (6)	0.0140 (6)	−0.0066 (5)	0.0100 (5)	−0.0036 (5)
C4	0.0191 (6)	0.0175 (6)	0.0103 (5)	0.0047 (5)	−0.0009 (5)	−0.0010 (4)
C5	0.0130 (5)	0.0163 (6)	0.0112 (5)	−0.0033 (4)	0.0012 (4)	−0.0052 (4)
C6	0.0351 (8)	0.0164 (6)	0.0128 (6)	0.0116 (6)	0.0029 (6)	−0.0020 (5)
C7	0.0135 (5)	0.0094 (5)	0.0130 (5)	0.0005 (4)	0.0005 (4)	−0.0011 (4)
C8	0.0152 (6)	0.0135 (6)	0.0148 (6)	0.0026 (5)	0.0000 (5)	−0.0001 (4)
C9	0.0134 (5)	0.0089 (5)	0.0120 (5)	−0.0001 (4)	−0.0002 (4)	−0.0005 (4)
C10	0.0149 (6)	0.0127 (6)	0.0141 (5)	−0.0018 (4)	0.0011 (4)	−0.0019 (4)
C11	0.0175 (6)	0.0181 (6)	0.0129 (6)	−0.0003 (5)	0.0019 (5)	−0.0042 (5)
C12	0.0255 (7)	0.0147 (6)	0.0154 (6)	−0.0023 (5)	−0.0018 (5)	−0.0047 (5)
C13	0.0204 (7)	0.0166 (6)	0.0211 (6)	−0.0063 (5)	−0.0026 (5)	−0.0042 (5)

Geometric parameters (Å, º)

Fe1—C1	2.0349 (12)	C2—C3	1.423 (2)
Fe1—C1^{i}	2.0349 (12)	C2—H2	0.9500
Fe1—C2	2.0453 (13)	C3—C4	1.413 (2)
Fe1—C2^{i}	2.0453 (13)	C3—H3	0.9500
Fe1—C5	2.0471 (13)	C4—C5	1.4145 (19)
Fe1—C5^{i}	2.0471 (13)	C4—H4	0.9500
Fe1—C4	2.0602 (13)	C5—H5	0.9500
Fe1—C4^{i}	2.0603 (13)	C6—H6A	0.9900
Fe1—C3	2.0614 (13)	C6—H6B	0.9900
Fe1—C3^{i}	2.0614 (13)	C7—C8	1.3837 (18)
N1—C8	1.3466 (19)	C7—C9	1.4646 (18)
N1—N2	1.3497 (19)	C8—H8	0.9500
N1—C6	1.4700 (18)	C9—C10	1.3987 (18)
N2—N3	1.3185 (17)	C10—C11	1.3838 (19)
N3—C7	1.3656 (18)	C10—H10	0.9500
N4—C13	1.3412 (19)	C11—C12	1.388 (2)
N4—C9	1.3435 (18)	C11—H11	0.9500
C1—C5	1.4248 (19)	C12—C13	1.382 (2)
C1—C2	1.4334 (19)	C12—H12	0.9500
C1—C6	1.4910 (19)	C13—H13	0.9500
C1—Fe1—C1^{i}	180.0	C5—C1—Fe1	70.03 (7)
C1—Fe1—C2	41.13 (5)	C2—C1—Fe1	69.83 (7)
C1^{i}—Fe1—C2	138.87 (5)	C6—C1—Fe1	124.11 (9)
C1—Fe1—C2^{i}	138.87 (5)	C3—C2—C1	107.90 (12)
C1^{i}—Fe1—C2^{i}	41.13 (5)	C3—C2—Fe1	70.34 (8)
C2—Fe1—C2^{i}	180.0	C1—C2—Fe1	69.04 (7)
C1—Fe1—C5	40.86 (5)	C3—C2—H2	126.0
C1^{i}—Fe1—C5	139.14 (5)	C1—C2—H2	126.0
C2—Fe1—C5	68.47 (5)	Fe1—C2—H2	126.1

C2^{i}—Fe1—C5	111.53 (5)	C4—C3—C2	108.01 (12)
C1—Fe1—C5^{i}	139.14 (5)	C4—C3—Fe1	69.90 (8)
C1^{i}—Fe1—C5^{i}	40.85 (5)	C2—C3—Fe1	69.12 (8)
C2—Fe1—C5^{i}	111.53 (5)	C4—C3—H3	126.0
C2^{i}—Fe1—C5^{i}	68.47 (5)	C2—C3—H3	126.0
C5—Fe1—C5^{i}	180.00 (7)	Fe1—C3—H3	126.5
C1—Fe1—C4	68.35 (5)	C3—C4—C5	108.52 (12)
C1^{i}—Fe1—C4	111.65 (5)	C3—C4—Fe1	69.99 (8)
C2—Fe1—C4	67.96 (6)	C5—C4—Fe1	69.36 (7)
C2^{i}—Fe1—C4	112.04 (6)	C3—C4—H4	125.7
C5—Fe1—C4	40.29 (6)	C5—C4—H4	125.7
C5^{i}—Fe1—C4	139.71 (6)	Fe1—C4—H4	126.5
C1—Fe1—C4^{i}	111.65 (5)	C4—C5—C1	108.24 (12)
C1^{i}—Fe1—C4^{i}	68.35 (5)	C4—C5—Fe1	70.36 (8)
C2—Fe1—C4^{i}	112.04 (6)	C1—C5—Fe1	69.11 (7)
C2^{i}—Fe1—C4^{i}	67.96 (6)	C4—C5—H5	125.9
C5—Fe1—C4^{i}	139.71 (6)	C1—C5—H5	125.9
C5^{i}—Fe1—C4^{i}	40.29 (5)	Fe1—C5—H5	126.2
C4—Fe1—C4^{i}	180.00 (8)	N1—C6—C1	112.79 (12)
C1—Fe1—C3	68.63 (5)	N1—C6—H6A	109.0
C1^{i}—Fe1—C3	111.37 (5)	C1—C6—H6A	109.0
C2—Fe1—C3	40.54 (6)	N1—C6—H6B	109.0
C2^{i}—Fe1—C3	139.46 (6)	C1—C6—H6B	109.0
C5—Fe1—C3	67.93 (6)	H6A—C6—H6B	107.8
C5^{i}—Fe1—C3	112.07 (6)	N3—C7—C8	108.55 (12)
C4—Fe1—C3	40.11 (6)	N3—C7—C9	122.77 (12)
C4^{i}—Fe1—C3	139.89 (6)	C8—C7—C9	128.62 (13)
C1—Fe1—C3^{i}	111.37 (5)	N1—C8—C7	104.22 (12)
C1^{i}—Fe1—C3^{i}	68.63 (5)	N1—C8—H8	127.9
C2—Fe1—C3^{i}	139.46 (6)	C7—C8—H8	127.9
C2^{i}—Fe1—C3^{i}	40.54 (6)	N4—C9—C10	122.94 (12)
C5—Fe1—C3^{i}	112.07 (6)	N4—C9—C7	115.54 (12)
C5^{i}—Fe1—C3^{i}	67.93 (6)	C10—C9—C7	121.50 (12)
C4—Fe1—C3^{i}	139.89 (6)	C11—C10—C9	118.52 (13)
C4^{i}—Fe1—C3^{i}	40.11 (6)	C11—C10—H10	120.7
C3—Fe1—C3^{i}	180.0	C9—C10—H10	120.7
C8—N1—N2	111.35 (11)	C10—C11—C12	119.08 (13)
C8—N1—C6	129.20 (14)	C10—C11—H11	120.5
N2—N1—C6	119.45 (13)	C12—C11—H11	120.5
N3—N2—N1	107.30 (12)	C13—C12—C11	118.35 (13)
N2—N3—C7	108.57 (12)	C13—C12—H12	120.8
C13—N4—C9	117.19 (12)	C11—C12—H12	120.8
C5—C1—C2	107.33 (12)	N4—C13—C12	123.89 (14)
C5—C1—C6	125.82 (13)	N4—C13—H13	118.1
C2—C1—C6	126.83 (14)	C12—C13—H13	118.1
C8—N1—N2—N3	0.31 (16)	N2—N1—C6—C1	88.89 (17)
C6—N1—N2—N3	−179.79 (12)	C5—C1—C6—N1	96.79 (18)

N1—N2—N3—C7	−0.34 (15)	C2—C1—C6—N1	−85.10 (18)
C5—C1—C2—C3	0.44 (14)	Fe1—C1—C6—N1	−174.35 (11)
C6—C1—C2—C3	−177.96 (12)	N2—N3—C7—C8	0.26 (16)
Fe1—C1—C2—C3	−59.84 (9)	N2—N3—C7—C9	−177.32 (12)
C5—C1—C2—Fe1	60.28 (9)	N2—N1—C8—C7	−0.15 (15)
C6—C1—C2—Fe1	−118.12 (13)	C6—N1—C8—C7	179.97 (13)
C1—C2—C3—C4	−0.26 (15)	N3—C7—C8—N1	−0.06 (15)
Fe1—C2—C3—C4	−59.29 (9)	C9—C7—C8—N1	177.33 (13)
C1—C2—C3—Fe1	59.03 (9)	C13—N4—C9—C10	0.0 (2)
C2—C3—C4—C5	−0.02 (15)	C13—N4—C9—C7	−178.92 (12)
Fe1—C3—C4—C5	−58.82 (9)	N3—C7—C9—N4	167.64 (13)
C2—C3—C4—Fe1	58.81 (9)	C8—C7—C9—N4	−9.4 (2)
C3—C4—C5—C1	0.29 (15)	N3—C7—C9—C10	−11.3 (2)
Fe1—C4—C5—C1	−58.92 (9)	C8—C7—C9—C10	171.60 (13)
C3—C4—C5—Fe1	59.21 (9)	N4—C9—C10—C11	1.4 (2)
C2—C1—C5—C4	−0.45 (14)	C7—C9—C10—C11	−179.75 (12)
C6—C1—C5—C4	177.97 (12)	C9—C10—C11—C12	−1.7 (2)
Fe1—C1—C5—C4	59.70 (9)	C10—C11—C12—C13	0.8 (2)
C2—C1—C5—Fe1	−60.15 (9)	C9—N4—C13—C12	−1.1 (2)
C6—C1—C5—Fe1	118.27 (13)	C11—C12—C13—N4	0.6 (2)
C8—N1—C6—C1	−91.24 (19)		

Symmetry code: (i) −*x*+1, −*y*+1, −*z*+1.

Hydrogen-bond geometry (Å, º)

D—H···*A*	*D*—H	H···*A*	*D*···*A*	*D*—H···*A*
C8—H8···N3^{ii}	0.95	2.68	3.601 (2)	163
C5—H5···N2^{ii}	0.95	2.51	3.4240 (19)	160
C3—H3···N4^{iii}	0.95	2.73	3.4625 (19)	135
C12—H12···Cp$_{centroid}^{iv}$	0.95	2.69	3.4861 (15)	142

Symmetry codes: (ii) *x*−1, *y*, *z*; (iii) *x*, *y*+1, *z*; (iv) −*x*+2, −*y*, −*z*.